

Short Communication

Nano-confined Synthesis of Highly Ordered Mesoporous Carbon and its Performance as Electrode Material for Electrochemical Behavior of Riboflavin (Vitamin B2) and Dopamine

Mohammad A. Wahab^{1*}Π, Farzana Darain²Π, M. A. Karim³, and Jorge N. Beltramini¹

¹Nanomaterials Centre (Nanomac), Australian Institute of Bioengineering and Nanotechnology (AIBN) of the University of Queensland, 75, Corner of College and Cooper Roads, St Lucia, Brisbane, QLD 4072, Queensland, Australia, Tel: + 61733464803;

²School of Chemistry and Molecular Biosciences of the University of Queensland, St Lucia, Brisbane, QLD 4072, Australia

³Chemistry, Physics and Mechanical Engineering, Science and Engineering Faculty, Queensland University of Technology, 2 George Street, QLD 4001 Australia.

Π Equal contribution to this paper.

*E-mail: m.wahab@uq.edu.au

Received: 18 March 2015 / Accepted: 22 May 2015 / Published: 28 July 2015

Highly ordered mesoporous carbon (MC) has been synthesized from sucrose, a non-toxic and cost-effective source of carbon. X-ray diffraction, N₂ adsorption–desorption isotherm and transmission electron micrograph (TEM) were used to characterize the MC. The XRD patterns show the formation of highly ordered mesoporous structures of SBA15 and mesoporous carbon. The N₂ adsorption-desorption isotherms suggest that the MC exhibits a narrow pore-size distribution with high surface area of 1559 m²/g. The potential application of MC as a novel electrode material was investigated using cyclic voltammetry for riboflavin (vitamin B2) and dopamine. MC-modified glassy carbon electrode (MC/GC) shows increase in peak current compared to GC electrode in potassium ferricyanide which clearly suggest that MC/GC possesses larger electrode area (1.8 fold) compared with bare GC electrode. The electrocatalytic behavior of MC/GC was investigated towards the oxidation of riboflavin (vitamin B2) and dopamine using cyclic voltammetry which show larger oxidation current compared to unmodified electrode and thus MC/GC may have the potential to be used as a chemically modified electrode.

Keywords: Highly ordered mesoporous carbon, cyclic voltammetry, riboflavin, dopamine

1. INTRODUCTION

In recent years, ordered mesoporous carbon with favourable characteristics including high specific surface area, large pore volume, uniform pores and its connectivity pores to pores and high mechanical and thermal stability have shown the potential applications in catalysis, energy storage, electrode materials, biomolecules adsorption and separation, sensor and biomedical devices [1-5,6-14]. Importantly, these mesoporous carbon can increase the electron transfer rate which has indicated the applications based on the fabrication of chemically modified electrodes for various biomolecules including dopamine, riboflavin, L-cysteine, and so on [6,15-18].

Dopamine is an important brain neurotransmitter molecule of catecholamine. It plays a crucial role in the function of central nervous, hormonal, renal and cardiovascular system [19,20]. Changes in the concentration of dopamine have impact on several diseases. Its deficiency leads to brain disorders named Parkinson's disease and the excess activity of dopamine can be related to Schizophrenia.²¹ Electrochemical behavior of dopamine plays important roles in its physiological functions, and is a key factor in diagnosis of some diseases in clinical medicine [22].

On the other hand, riboflavin known as vitamin B2 a water-soluble compound, is also very essential for cell growth and it also plays potential cofactor in enzymes for general human health [23-30]. It is also a well-known biochemical product that could be found in food and pharmaceutical products and ranged from single vitamin to multivitamin formulations for the treatment of vitamin B2 deficiency in living body. The core structure of riboflavin an isoalloxazine ring, participates in enzyme-catalyzed electron transfer processes of many important metabolites in biological systems [1-6,23-30]. Therefore, it is very important to investigate electrochemical behavior of riboflavin to develop methods for finding its physiological functions in clinical medicine and biological systems [26-30].

The electrochemical technique becomes important in the analysis of electroactive biochemical compounds. So far, very limited reports on the electrochemical studies for riboflavin and dopamine have been reported based on solid-electrode systems using highly ordered mesoporous carbon as an electrode materials, although the large surface area and the presence of edge plane-like sites on highly ordered mesoporous carbon structures could contribute for enhancing the oxidation and detection riboflavin and dopamine [2,3,6,28,30-32].

In this paper, highly ordered mesoporous carbon material (MC) was synthesized *via* impregnation of SBA15 nano-hard template with sucrose source and characterized with XRD, TEM, and BET. Then, the performance of MC as an electrode material was investigated using cyclic voltammetry. The MC was employed to modify glassy carbon electrode for electrochemical studies of riboflavin and dopamine in phosphate buffer, pH 7.0.

2. EXPERIMENTAL

2.1 Materials

Tetraethylorthosilicate (TEOS), Poly(ethylene oxide)-poly(propylene oxide)-poly(ethylene oxide) triblock copolymer Pluronic surfactant P123 (EO₂₀PPO₇₀EO₂₀), and sucrose from Sigma-

Aldrich were used as reagent for this work. In addition, diluted HF, HCl and other solvents were also used as received. Riboflavin (RB) and dopamine (DA) were received from ICN Biomedical Inc. and Sigma, respectively. The phosphate buffer solutions (0.1 M PBS, pH 7.0 was prepared by mixing standard solutions of NaH_2PO_4 (Sigma) and Na_2HPO_4 (Sigma). DA and RB were used as freshly prepared.

2.2 Synthesis of mesoporous SBA15 Silica nano-hard template

At first, high ordered SBA-15 silica nano-hard template was synthesized using the triblock copolymer, Pluronic P123 as structure directing agent and tetraethyl orthosilicate (TEOS) as the silica source. For preparing SBA15, 2 g of surfactant P123 was added to 60 mL of 2M HCl at 38 °C and vigorous stirring was continued at least for 2h. Then 4.2 g of TEOS was added drop by drop to the surfactant containing acidic solution under vigorous stirring [14,34]. The solution mixture was then vigorously stirred for 8 min and left for 24 h at 38 °C. Afterwards it was transferred into autoclave at 100 °C for another 24 h. The as-synthesized SBA-15 silica was collected by filtration, dried at room temperature and then calcined at 550 °C for 6 h in air with heating rate 5°C/min.

2.2.1 Nano-confined synthesis of highly ordered mesoporous carbon (MC)

The synthesis of ordered mesoporous carbon (MC) was carried out by using above synthesized SBA15 silica nano-hard template, following the procedure reported elsewhere [14]. The calcined SBA-15 was impregnated/nano-confined with aqueous solution of sucrose containing sulphuric acid. Briefly, 1.0 g of calcined SBA15 silica template was added slowly to a solution obtained by dissolving 1.25 g of sucrose as a carbon source and 0.14 g of H_2SO_4 in 5 g of water. This mixture was stirred for few hours until homogenous solution formed. The mixture was placed in a drying oven for 6 h at 100 °C for 6 h and subsequently the oven temperature was increased to at 160 °C and held again for another 6 h. The sample turned dark brown / black during the heat treatment process in the oven. The silica sample, containing partially polymerized and carbonized sucrose at the present step, was treated again at 100 °C and 160 °C using the same drying oven after the incorporation of 0.8 g of sucrose, 0.09 g of H_2SO_4 and 5 g of water [14]. The carbonization was carried out with heating to typically 850 °C under an argon atmosphere. For removing the silica template, the carbonized sample was washed with 5-7% HF solution at room temperature for overnight. The silica template-free highly ordered mesoporous carbon thus obtained was filtered, washed with ethanol, and dried at 100 °C K.

2.2.2. Electrode preparation and electrochemical measurements

Prior to the electrode preparation, the MC was pre-dried at 60°C for 1 h in a conventional oven. 5 mg of MC was dispersed in 20 ml of ethanol and then sonicated for 30 min to obtain a black suspension. The bare glassy carbon (GC) electrode was polished with 0.50 and 0.05 μm alumina slurry and then rinsed with water. The electrode was then sonicated in water for 5 min and dried under high

purity nitrogen stream. The MC was dispersed in ethanol and ultrasonicated for 20 min to ensure good dispersion and homogeneity in ethanol. Then, 4 μL of MC suspension was drop-casted on the cleaned GC and dried under nitrogen atmosphere to obtain a MC/GC electrode.

Electrochemical experiments were performed on a Bioanalytical Systems BAS 100B/W electrochemical workstation with three-electrode system comprising of a modified GC as working electrode, Ag/AgCl as reference electrode and platinum as counter. A 0.1M phosphate buffer solution (PBS, pH 7.0) was used as the supporting electrolyte for the potential cycling of potassium ferricyanide, $\text{K}_3\text{Fe}(\text{CN})_6$, dopamine, and riboflavin. All experimental solutions were deoxygenated by purging pure N_2 into the solution for about 15 min, and N_2 gas was kept flowing as a blanket over the solution during the electrochemical measurements. All electrochemical experiments were carried out at room temperature.

2.2.3. Characterization

XRD patterns were recorded with a Bruker radiation D8 Advanced Diffractometer with $\text{Cu K}\alpha$ radiation for angles 1 to 10 2θ (degree), whereas a Rigaku Miniflex diffractometer (Japan) with $\text{Cu K}\alpha$ radiation was used for the 2θ range from 10 to 80° under identical conditions at a scanning rate of 2 degree. An automated adsorption analyzer (Quadrachrome SI, Quantachrome, USA) was employed to measure the Brunauer–Emmett–Teller (BET) surface areas and textural properties. Before this measurements, all samples were outgassed for 12 h at 180°C in the degas port of the adsorption analyser [35,36]. The pore-size distribution (PSD) was obtained using the Barrett-Joyner-Halenda (BJH) model from the desorption branch [35,36]. For pore morphology observation, MC sample is ultrasonically dispersed in ethanol. TEM (TEM, FEI Tecnai 20, 200kV) imaging was carried out on a F20 microscope with an accelerating voltage 200 kV.

3. RESULTS AND DISCUSSION

Fig. 1 shows comparison of XRD patterns of calcined mesoporous SBA15 silica template and its mesoporous carbon replica. The XRD pattern of the mesoporous carbon replica shows three well-resolved reflections that could be assigned to (100), (110), and (200) reflections of the 2-D hexagonal materials, indicating a retention of the ordered structure of its host SBA15 host [6,14,37-42]. The cell parameter of the MC replica is smaller than that of the host SBA-15 silica template, due to the shrinkage of the carbon/silica composite material during pyrolysis and dissolution of host silica [41]. The higher angle XRD pattern of the MC (inset in Figure 1) shows two distinguished broad peaks, supporting the formation of graphitic carbon nature in the final structure [27,34]. The nitrogen adsorption-desorption isotherms of mesoporous SBA15 silica template and its mesoporous carbon replica are shown in Fig. 2 [14,40]. The N_2 adsorption-desorption isotherms of mesoporous SBA15 silica template in Fig. 2 are of type IV, [6,37-42] with the capillary condensation step at relative pressure of 0.61 to 0.8, corresponding to the existence of ordered mesopores with a narrow pore size distribution. On the other hand, MC replica shows the isotherm that shows a step at relative pressure

between 0.35 and 0.50, suggesting a narrow pore-size distribution. PSD data seen in Fig. 3 confirms this distinct behavior of mesoporous carbon structure.

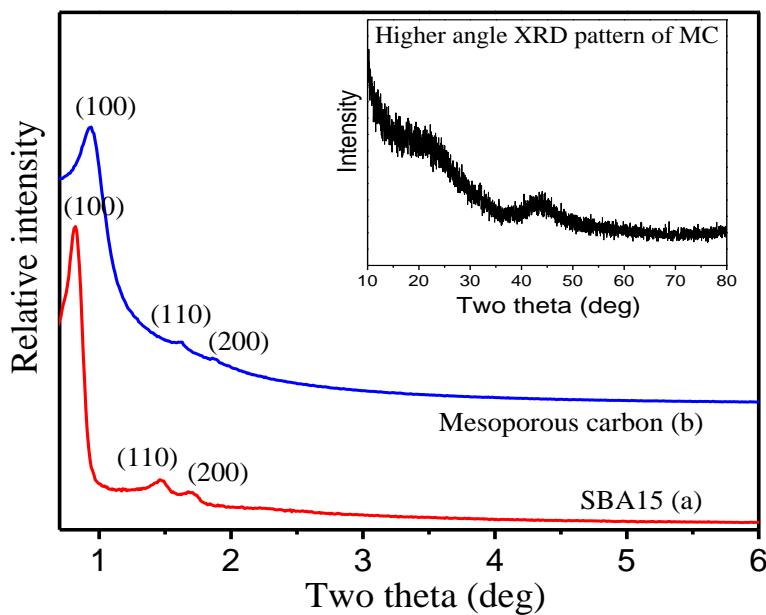


Figure 1. (a) XRD patterns of calcined SBA-15 and (b) the mesoporous carbon (MC) replica. The inset shows the higher angle XRD pattern of the MC replica.

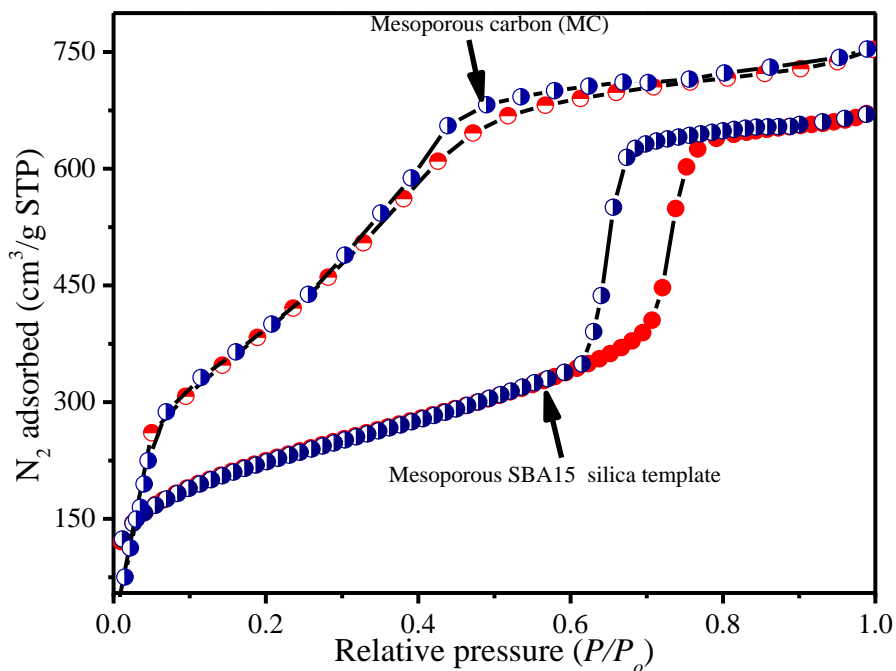


Figure 2. N₂ adsorption-desorption isotherms of SBA15 and mesoporous carbon. Sample names are already shown in Figure 2.

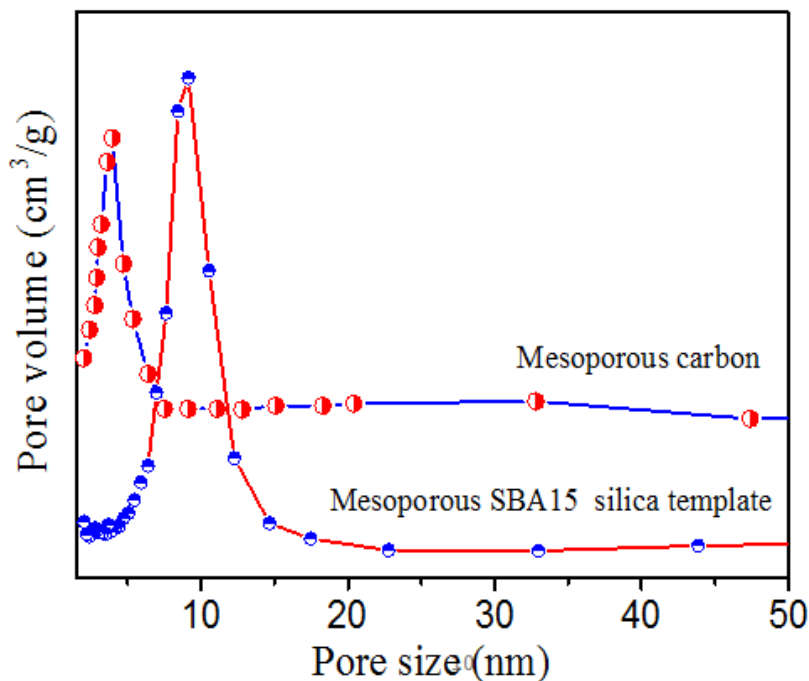


Figure 3. Pore size distribution of SBA15 and mesoporous carbon. Sample names are already included in Figure.

As shown in Fig. 3, the pore size of MC is about 3.95 nm, whereas pore size of SBA15 is about 9.15 nm. The specific BET surface area and a total pore volume of the SBA15 are 719 m²/g and 1.12 cm³/g, respectively, whereas MC shows a very high BET surface area of 1559 m²/g and a large total pore volume of 1.6 cm³/g. The total large pore volume of MC is usually related to the volume of the ordered pores with minor contribution from micropores and possibly also from secondary mesopores [14]. The hysteresis does not close at high relative pressure because of formation of interparticle textural pores in the MC structure. Pore structure of MC is investigated by TEM image in Fig. 4. TEM image in Fig. 4 clearly shows TEM image for MC viewed along and perpendicular to the direction of the hexagonal pores. It is found that pores are interconnected, which are constituted by the carbon that filled the channel-interconnecting micropores within the SBA-15 wall [37-42].

The potential application of MC/GC in electrochemistry as a novel electrode material was investigated using potassium ferricyanide (K₃[Fe(CN)₆]). As shown in Fig. 5, the redox peak currents of potassium ferricyanide (1 mM prepared in 0.1M PBS, pH 7.0) at the MC/GC electrode (solid line) was much higher compared to GC electrode (dotted line). This phenomenon suggests that MC-modified GC electrode possesses larger electrode area as compared with bare GC electrode. The electroactive surface area of MC/GC and GC electrodes can be obtained from the Randles–Sevcik equation [43].

$$i_p = (2.69 \times 10^5) AD^{1/2} n^{3/2} v^{1/2} c^* \quad (1)$$

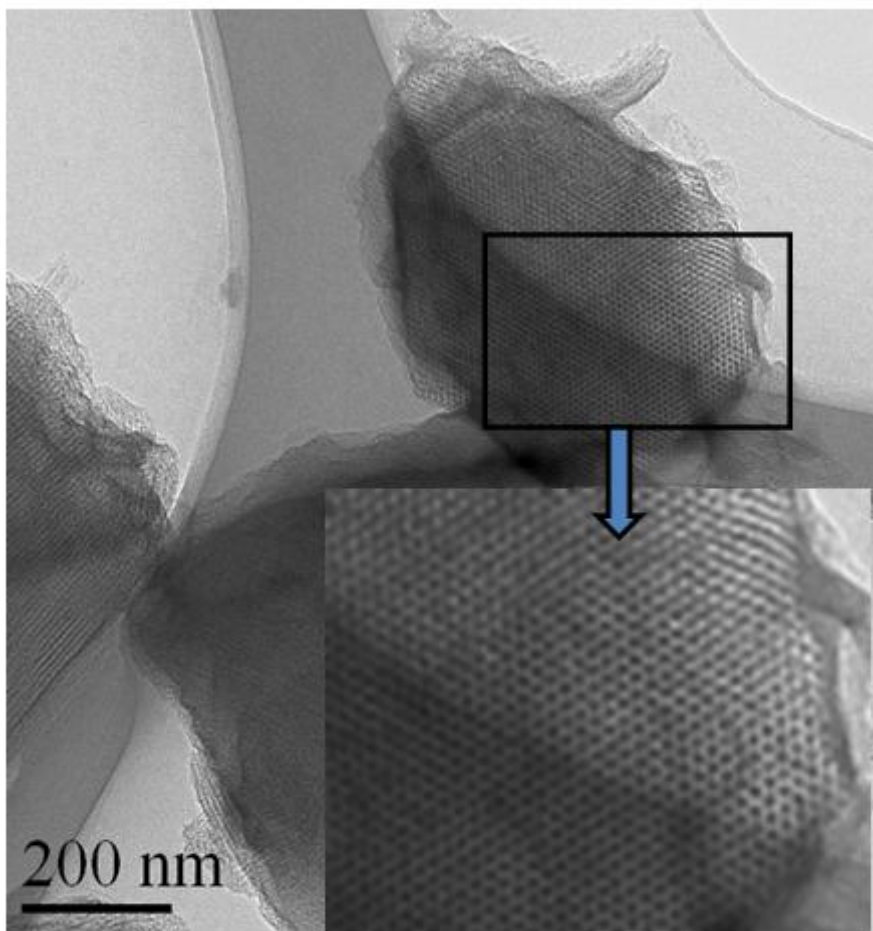


Figure 4. TEM image of the highly ordered mesoporous carbon (MC).

where i_p is the peak current (A), n is the number of electrons participating in the redox reaction, A is the electroactive surface area (cm^2) of the electrode, D is the diffusion coefficient of $[\text{Fe}(\text{CN})_6]^{3-}$ (taken to be $7.60 \times 10^{-6} \text{ cm}^2 \text{ s}^{-1}$ in aqueous medium), the molecule in solution ($\text{cm}^2 \text{ s}^{-1}$), c^* corresponds to the bulk concentration of the redox probe (mol cm^{-3}), and ν is the scan rate (V/s). According to the equation, the electroactive surface area for MC/GC electrode is 0.053 cm^2 , which is significantly higher (around 1.8 times higher) than that of a GC electrode (0.029 cm^2), suggesting that the MC/GC electrode possesses larger effective surface area. The peak potential separation (ΔE_p) between the anodic and cathodic peaks is 54 mV for the MC/GC electrode and 72 mV for GC electrode. The decrease in ΔE_p , **indicated** that the MC/GC electrode not only possesses high surface area but also accelerates the electron transfer rate of ferricyanide. These results show that the MC/GC electrode has relatively better electrochemical activity. So, MC can be used as a new potential material for this analytical application.

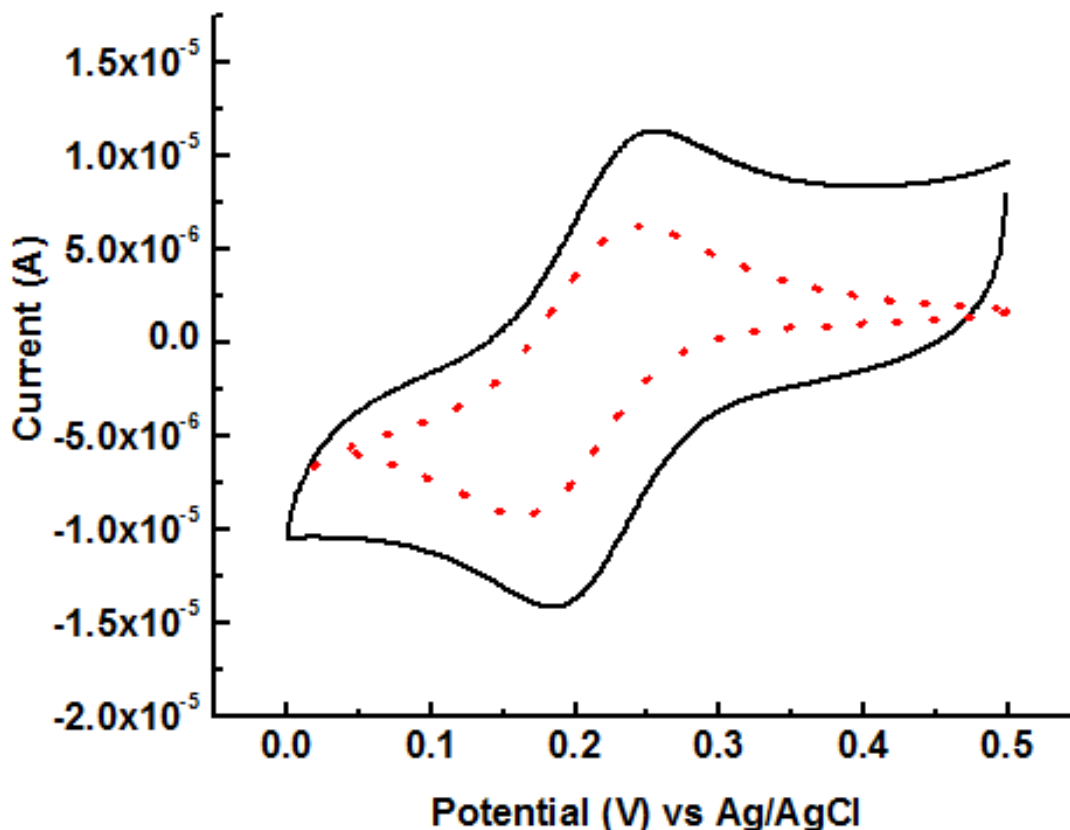


Figure 5. MC/GC (solid line) and GC (dotted line) in 1 mM $K_3Fe(CN)_6$ (prepared in 0.1M PBS, pH 7.0) at 10 mV/s

The response of MC/GC electrode (solid line) and bare GC electrode (dotted line) towards riboflavin and dopamine were investigated and compared in phosphate buffer solution, pH 7.0 as depicted in Fig. 6. Fig. 6A shows the CVs obtained for riboflavin in which, the potential range was controlled between -0.75 and +0.5 V vs. Ag/AgCl. A pair of redox peak which corresponds to a reversible reduction and oxidation process was observed for both bare GC and MC/GC electrodes. The separation between peak potential (ΔE_p) for bare GC and MC/GC electrodes were found to be around -430 mV and -400 mV vs. Ag/AgCl, respectively. However, the peak currents are significantly higher for the MC/GC electrode compared to bare GC electrode, under the same measurement conditions (Fig 6A, solid line), which indicates that the reversibility of riboflavin was greatly enhanced by the use of mesoporous carbon as electrode material coated on GC. This observation is consistent with previous reports [6,43]. Fig. 6B presents the CVs obtained for MC/GC and bare GC electrodes in dopamine solution. For bare GC electrode, oxidation peak was observed at around 570 mV vs. Ag/AgCl. One can notice that the CV peak for the oxidation of dopamine at a MC/GC has been shifted to negative potential compared to GC electrode. For the same measurement condition, the oxidation peak for MC/GC electrode was appeared at around 230 mV vs. Ag/AgCl. Furthermore, the anodic peak current on the MC/GC was significantly higher than that of bare GC in same dopamine solution (Fig. 6B solid line) which reveals that mesoporous carbon material has a better electrocatalytic effect on dopamine. Similar observation was reported in the literatures [6,42-44]. The superiority in analytical performance

of the mesoporous carbon materials coated GC electrode over the bare GC electrode might be ascribed to the fact that mesoporous carbon materials can provide higher electrical conductivity, enlarged/high active surface areas, uniform and larger pore volume, surface roughness, and more coordinate sites to the interface so it can enhance current that appears for a typical electrocatalytic response for riboflavin and dopamine.

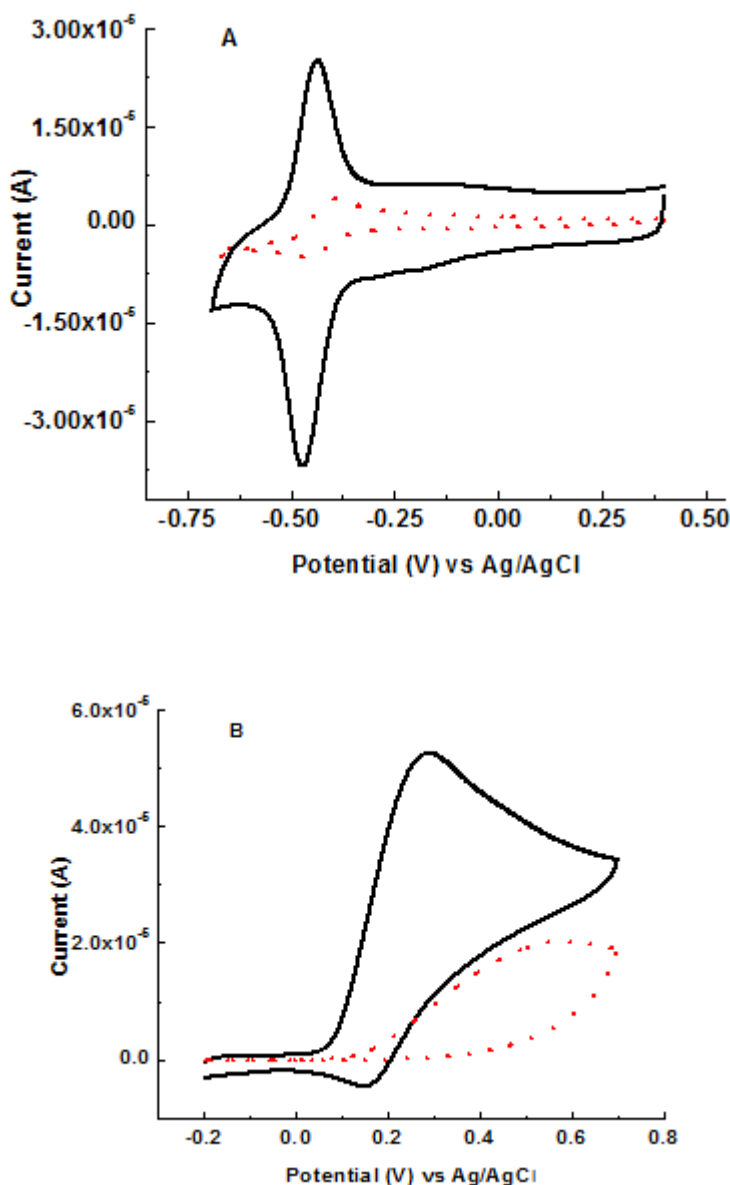


Figure 6. A. MC/GC (solid line) and GC(dotted line) in 1 mM riboflavin prepared in 0.1 M PBS, pH 7.0 at 20 mV/s; B. MC/GC (solid line) and GC(dotted line) in 1 mM dopamine prepared in 0.1 M PBS, pH 7.0 at 20 mV/s.

4. CONCLUSIONS

In summary, we have clearly demonstrated here that a highly ordered mesoporous carbon materials (MC) synthesized from sucrose carbon source can have great potential to be used as electrode material. It is evident from this study that MC-modified electrode showed faster electron

transfer and higher current response compared to bare glassy carbon electrode. Moreover, the MC-modified electrode showed high electrocatalytic activity towards the oxidation of riboflavin and dopamine. Therefore, MC, with its high surface area and, large pore volume might be used as a chemically modified electrode to explore electroanalytical applications.

ACKNOWLEDGEMENT

Authors thank the ARC Centre and AIBN-UQ providing the new staff grant and research fund and facilities at ARC Centre for Functional Nanomaterials, AIBN UQ. We acknowledge the facilities and the scientific and technical assistance of the Australian Microscopy and Microanalysis Research Facility at the Centre for Microscopy and Microanalysis, University of Queensland, Brisbane, Australia.

References

1. B. Janik, P.J. Elving, *Chem. Rev.* 68 (1968) 295-319.
2. K.K. Shiu, K. Shi, *Electroanalysis* 12 (2000) 134-139.
3. H.Y. Gu, A.M. Yu, H.Y. Chen, *Anal. Lett.* 34 (2001) 2361-2374.
4. N.R. Vettorazzi, L. Sereno, M. Katoh, *J. Electrochem. Soc.* 155 (2008) F110-F115.
5. R.G. Compton, J.S. Foord, F. Marken, *Electroanalysis* 15 (2003) 1349-1418.
6. J. Bai, N.J. Chrysostome, L. Liu, L. Yang, L. Guo, *J. Solid-State Electrochem.* 14 (2010) 2251-2256.
7. S.H. Joo, S.J. Choi, I. Oh, J. Kwak, Z. Liu, O. Terasaki, R. Ryoo, *Nature* 412 (2001) 169-172.
8. C.D. Liang, S. Dai, G. Guiochon, *Anal. Chem.* 75 (2003) 4904-4912.
9. P. Simon, Y. Gogotsi, *Nature Mater.* 7 (2008) 845-854.
10. J.B. Park, J. Lee, C.S. Yoon, Y.K. Sun, *ACS Appl. Mater. Interfaces* 5 (2013) 13426-13431.
11. C. You, Y. Xuewu, Y. Wang, S. Zhang, J. Kong, D. Zhao, B. Liu, *Electrochem. Commun.* 11 (2009) 227-230.
12. T.P. Fellingner, F. Haschee, P. Strasser, M. Antonietti, *J. Am. Chem. Soc.* 134 (2012) 4072-4075.
13. H. Hosseini, M. Behbahani, M. Mahyari, H. Kazerooni, A. Bagheri, A. Shaabani, *Biosens. Bioelectron.* 59 (2014) 412-417.
14. M.A. Wahab, Y. Jia, D. Yang, H. Zhao, X.D. Yao, *J. Mater. Chem. A.* 1 (2013) 3471-3478.
15. M. Zhou, J. Ding, L.P. Guo, Q. K. Shang, *Anal. Chem.* 79 (2007) 5328-5335.
16. M. Zhou, L. Shang, B.L. Li, L.J. Huang, S.J. Dong, *Electrochem. Commun.* 10 (2008) 859-863.
17. N. Q. Jia, Z. Y. Wang, G. F. Yang, H. B. Shen and L. Z. Zhu, *Electrochem. Commun.*, 9 (2007) 233-238.
18. J.J. Yu, D.L. Yu, T. Zhao, B. Z. Zeng, *Talanta* 74 (2008) 1586-1591.
19. P. Damier, E.C. Hirsch, Y. Agid, A.M. Graybiel, *Brain* 122 (1999) 1437-1448.
20. J.R. Cooper, F.E. Bloom, R.H. Roth, *The Biochemical Basis of Neuropharmacology*; Oxford University Press, New York, (1986).
21. R.M. Wightman, L.J. May, A.C. Michael, *Anal. Chem.* 60 (1988) 769A-779A.
22. J.A. Stamford, J.B. Justice, *Anal. Chem.* 69 (1996) 359A-363A.
23. W. Friedrich, *Vitamins. Walter de Gruyter*, Berlin, (1988) 404-409.
24. F. Müller, *Chemistry and Biochemistry of Flavoenzymes*, vol. 1. CRC, Boca Raton, 1991.
25. P.F. Heelis, *Chem. Soc. Rev.* 11 (1982) 15-39.
26. E. Silva, A.M. Edwards, in *Flavins, Photochemistry and Photobiology, Comprehensive Series in Photochemistry and Photobiology*, vol. 6. The Royal Society of Chemistry, Cambridge, (2006)
27. J. Ghasemi, B. Abbasi, A. Niazi, E. Nadaf, A. Mordai, *Anal Lett.* 37 (2004) 2609-2623.

28. A. Chatterjee, J.S. Foord, *Diamond & Related Materials* 18 (2009) 899–903.
29. H. Horton, L. Moran, R. Ochs, J. Rawn, K. Scrimgeour, *Principles of Biochemistry*, Prentice Hall, (1996).
30. H.A.O. Hill, *Coord. Chem. Rev.* 151 (1996) 115–123.
31. T.R.I. Cataldi, D. Nardiello, V. Carrara, R. Ciriello, G.E.D. Benedetto, *Food Chem.* 82 (2003) 309–314.
32. J. Wang, D.B. Luo, P.A.M. Farias, J.S. Mahmoud, *Anal. Chem.* 57 (1985)158–162.
33. A. Economou, P.R. Fielden, *Electroanalysis* 7 (1995) 447–453.
34. C. Yu, J. Fan, B. Tian, D.Y. Zhao, *Chem Mater.* 16 (2004) 889–898.
35. S. Brunauer, P.H. Emmett, E. Teller, *J. Am. Chem. Soc.* 60 (1938) 309–318.
36. E.P. Barrett, L.G. Joyner, P.P. Halenda, *J. Am. Chem. Soc.* 73 (1951) 373–380.
37. N.Q. Jia, Z.Y. Wang, G.F. Yang, H.B. Shen, L.Z. Zhu, *Electrochem. Commun.* 9 (2007) 233–238.
38. D. S. Dhawale, M. R. Benzigar, M. A. Wahab, C. Anand, S. Vargghese, V. V. Balasubramanian, S. S. Aldeyab, K. Ariga, *Electrochemical Acta* 77 (2012) 256–261.
39. M.A. Wahab, F. Darain, *Nanotechnology* 25 (2014) 165701–165708.
40. C.M. Yang, C. Weidenthaler, B. Spliethoff, M. Mayanna, F. Schuth, *Chem. Mater.* 17 (2005) 355–358.
41. D. Zhao, Q. Huo, J. Feng, B. F. Chmelka, G.D. Stucky, *J. Am. Chem. Soc.*, 120 (1998) 6024–6036.
42. A. Bard, L.R. Faulkner, in *Electrochemical Methods—Fundamentals and Application*. Wiley, New York (2000).
43. M. Jafarian, F. Forouzandeh, I. Danaee, F. Gobal, M.G. Mahjani, *J Solid-State Electrochem.* 13 (2009) 1171–1179.
44. N. Jia, Z. Wang, G. Yang, H. Shen, L. Zhu, *Electrochem. Commun.* 9 (2007) 233–238.

© 2015 The Authors. Published by ESG (www.electrochemsci.org). This article is an open access article distributed under the terms and conditions of the Creative Commons Attribution license (<http://creativecommons.org/licenses/by/4.0/>).